Detection of Up-converted Persistent Luminescence in the Near Infrared Emitted by the $Zn_3Ga_2GeO_8:Cr^{3+}$, Yb^{3+}, Er^{3+} Phosphor

Feng Liu,[1,2] Yanjie Liang,[1,3] and Zhengwei Pan[1,2,*]
[1]College of Engineering, University of Georgia, Athens, Georgia 30602, USA
[2]Department of Physics and Astronomy, University of Georgia, Athens, Georgia 30602, USA
[3]Key Laboratory for Liquid-Solid Structure Evolution and Processing of Materials, Shandong University, Jinan 250061, China
(Received 9 May 2014; published 21 October 2014)

Up-conversion luminescence and long-persistent luminescence are two well-studied, special luminescence processes. By combining the unique features of these two luminescence processes, here we design a new luminescence process called up-converted persistent luminescence (UCPL), which enables us to generate persistent luminescence having an emission energy higher than the excitation energy. Guided by the UCPL concept, we create the first UCPL phosphor $Zn_3Ga_2GeO_8:1\%Cr^{3+}$, $5\%Yb^{3+}$, $0.5\%Er^{3+}$ by incorporating an up-converting ion pair Yb^{3+}/Er^{3+} into a $Zn_3Ga_2GeO_8:1\%Cr^{3+}$ near-infrared persistent phosphor. After being excited by a 980 nm laser, the phosphor emits long-lasting (>24 h) near-infrared persistent emission peaking at 700 nm. The UCPL concept and the associated phosphors are expected to have important implications for several fields such as biomedical imaging.

DOI: 10.1103/PhysRevLett.113.177401 PACS numbers: 78.60.-b, 42.65.Ky, 72.20.Jv, 78.55.Qr

Up-conversion luminescence (UCL) is a nonlinear optical process that converts low-energy excitation, usually at near-infrared (NIR) wavelengths, to higher-energy emission, typically in the visible spectral region [1]. As the hypothetical energy level scheme illustrated in the left panel of Fig. 1 shows, under the excitation of low-energy light, the ion system is excited from the ground state (G) to a high-energy excited state via an intermediate metastable state (M). Subsequently, after nonradiative relaxation, the excited ion from the emitting state (E) directly returns to the G state, accompanied with light emission that has higher energy than the excitation light. In conventional UCL materials, trivalent lanthanide ions such as Er^{3+}, Tm^{3+}, or Ho^{3+} are typically used as activator ions, owing to their ladderlike arranged energy levels that promote the absorption and transfer of photons [2]. Yb^{3+} ions, which have a sufficient absorption cross section in the NIR region, are often codoped as sensitizer ions to enhance the UCL efficiency by absorbing incident NIR photons and then transferring the accumulated excitation energy to the activator ions [2]. Efficient up-conversion emissions have been achieved in some fluorides (e.g., $NaYF_4:Yb^{3+}$, Er^{3+} [3]) and oxides (e.g., $YbPO_4:Er^{3+}$ [4]) in the forms of crystals or glasses [5–7].

Long-persistent luminescence (LPL) is a "self-sustained" luminescence phenomenon whereby luminescence can last for minutes to hours at room temperature after the stoppage of the excitation [8]. This process can be qualitatively explained by a simple schematic model based on an electron transfer assumption [9], as shown in the right panel of Fig. 1. Under excitation with ionizing radiation, the ion system is excited to a delocalized state (D; i.e., an excited state associated with delocalization properties). The delocalized electron may be captured by and stored in electron traps, which are generally lattice defects or impurities [10]. After ceasing the excitation, the captured electron may escape back to the D state owing to thermal stimulation or quantum tunneling, followed by nonradiative relaxation to the E state and then radiative return to the G state, accompanied with LPL emission. Because of the high energy of the trap level, the LPL process requires a high excitation energy [usually ultraviolet (UV) or blue light], which is higher than the energy of the emission light. Up to now, there have been persistent phosphors for each of the main emitting colors, as well as for the NIR spectral region, with representative ones including $CaAl_2O_4:Eu^{2+}$, Nd^{3+} (blue) [11], $SrAl_2O_4:Eu^{2+}$, Dy^{3+} (green) [12], $Y_2O_2S:Eu^{3+}$, Mg^{2+}, Ti^{4+} (red) [13], and $Zn_3Ga_2Ge_2O_{10}:Cr^{3+}$ (NIR) [14].

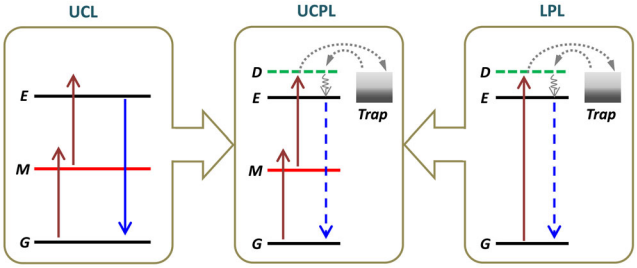

FIG. 1 (color online). Schematic diagrams of up-conversion luminescence (UCL), up-converted persistent luminescence (UCPL), and long-persistent luminescence (LPL), with hypothetical energy level schemes. G, M, E and D represent the ground state, metastable state, emission state, and delocalized state, respectively. Straight-line arrows and curved-line arrows represent optical transitions and electron transfer processes, respectively.

Although the UCL and LPL processes exhibit different luminescence forms and mechanisms, they share similar implications for a variety of technologies. In particular, both UCL nanophosphors and NIR LPL nanophosphors have attracted enormous attention in recent years for use as optical nanoprobes in biomedical imaging applications, because the involvement of high-penetrating NIR light as either an excitation source (for UCL [15–17]) or an imaging signal (for NIR LPL [18–20]) can greatly reduce the optical interference (e.g., tissue autofluorescence) from tissues, enabling significantly improved imaging sensitivity and depth. However, both the UCL and the LPL processes suffer from their own drawbacks. In UCL-based imaging, the need for real-time, intense NIR light excitation (typically a 980 nm NIR laser) can cause constant background noise that inevitably reduces the signal-to-noise ratio and, therefore, the object detectability. The detectability can be further reduced by the scattering and absorption of the generally short-wavelength light (usually in the visible spectral region) generated in the UCL process. In NIR LPL-based imaging, while the technique offers excitation-free and hence noise-free imaging conditions [18], its application is restricted by its short observation window, typically less than a few hours, which is insufficient for *in vivo* cell tracking, which needs a window of days or even weeks [21]. Since LPL materials are mostly effective with UV light excitation, which has short tissue penetration and is harmful to normal tissue, it is not possible to recharge the nanoprobes once they are inside a living subject. Thus, to make NIR LPL materials competitive in biomedical imaging, the nanoprobes need to be able to be effectively charged *in vivo* by a high-tissue-penetrating light source such as a 980 nm NIR laser.

The UCL and LPL diagrams in Fig. 1 suggest that the drawbacks of the UCL and LPL processes in biomedical imaging could possibly be overcome by combining the unique features of these two processes. We therefore propose a new conceptual luminescence process called up-converted persistent luminescence (UCPL) by combining the UCL and LPL processes, as illustrated in the middle panel of Fig. 1. According to this UCPL concept, the low-energy incident photons can promote the ion system from the ground state to the high-energy delocalized state via an up-conversion excitation channel, followed by filling of the traps. When the stored excitation energy is gradually released, a NIR persistent luminescence signal with higher energy can be generated. The net effect of the UCPL process is that persistent emission can be created by excitation energy that is lower than the emission energy, a phenomenon that does not occur in nature.

To justify the UCPL concept, we designed and fabricated a new material by incorporating the up-converting ion pair Yb^{3+}/Er^{3+} (5 mol%/0.5 mol%) into a NIR LPL phosphor $Zn_3Ga_2GeO_8:1\%Cr^{3+}$, forming the first UCPL phosphor $Zn_3Ga_2GeO_8:1\%Cr^{3+}$, $5\%Yb^{3+}$, $0.5\%Er^{3+}$ (hereafter referred to as ZGGO:Cr, Yb, Er). $Zn_3Ga_2GeO_8:1\%Cr^{3+}$ was chosen as the bench material because of its superior NIR LPL performance and its wide excitation range (from UV to red light) for LPL emission [14]. The ZGGO:Cr, Yb, Er phosphor was synthesized by a solid-state reaction method. Stoichiometric amounts of ZnO, Ga_2O_3, GeO_2, Cr_2O_3, Yb_2O_3, and Er_2O_3 powders were ground to form a homogeneous fine powder suitable for prefiring. The mixed powder was then prefired at 900 °C in air for 2 h. The prefired powder was pressed into disks using a hydraulic press, and then sintered at 1310 °C in air for 1.5 h to obtain the products. The crystal structure of the as-synthesized ZGGO:Cr, Yb, Er phosphor was measured using a PANalytical X'Pert PRO powder x-ray diffractometer with Cu $K\alpha_1$ radiation ($\lambda = 1.5406$ Å). The optical properties of the material were carefully studied using an array of spectral methods. A Horiba FluoroLog-3 spectrofluorometer, equipped with a 450 W xenon arc lamp, a R928P photomultiplier tube (240–850 nm), and a liquid nitrogen-cooled DSS-IGA020L InGaAs detector (800–1600 nm), was used to record the photoluminescence spectra, UCL spectra, decay curves, and LPL and UCPL emission spectra. A tunable 980 nm laser diode module (output power, 1–1000 mW) was used as the excitation source, whose output beam was not focused and had a spot size of about 20 mm^2. A homemade thermoluminescence (TL) measurement setup (temperature range, –196 to 300 °C; heating rate, 4 °C/s) was used to measure the TL properties. The variables used in the TL measurements included varied excitation energies (300–720 nm and 980 nm), and varied excitation powers (200–700 mW from the 980 nm laser; the corresponding power densities were about 1–3.5 W/cm^2), and varied excitation durations (10–1000 s). The delay time between the illumination and TL measurement was 1 min. An ITT PVS-14 Generation III night vision monocular was used to take the NIR images through a Pentax digital SLR camera that was connected to the eyepiece of the monocular. Before all the spectral measurements, the samples were heat treated in a muffle oven at 400 °C for 20 min to completely empty the electron traps. Appropriate optical filters were used to avoid stray light in all spectral measurements.

X-ray diffraction analyses show that the addition of the 5 mol%/0.5 mol% Yb^{3+}/Er^{3+} ion pair into $Zn_3Ga_2GeO_8:1\%Cr^{3+}$ does not affect the material's crystal structure (see Fig. S1 in the Supplemental Material [22]). Figure 2(a) illustrates the UCPL process in the ZGGO:Cr, Yb, Er system. Upon excitation in the $^2F_{5/2}$ level of the Yb^{3+} ions under 980 nm light, energy is transferred to the Er^{3+} ions, resulting in Er^{3+} in the $^4S_{3/2}$ and $^4F_{9/2}$ excited states via up conversion [1]. The $^4T_2/^2E$ excited states of Cr^{3+} are then populated via energy transfer from Er^{3+} to Cr^{3+} [23]. Besides the photoluminescence emission from Cr^{3+}, the up-converted excitation of Cr^{3+} will also lead to the filling of the traps (the traps can be filled after the excitation of all

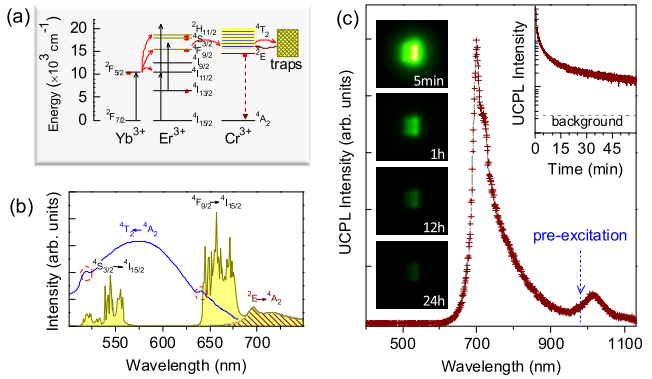

FIG. 2 (color online). (a) UCPL schematic diagram in the ZGGO:Cr, Yb, Er system. The straight-line arrows and curved-line arrows represent optical transitions and energy (or electron) transfer processes, respectively. The emission levels are marked with red solid spots. (b) UCL emission spectrum (curve with yellow shadow) under a 980 nm laser excitation and photoluminescence excitation spectrum of Cr^{3+} (blue solid-line curve) by monitoring the 700 nm emission. The red dashed-line circles indicate the positions of the characteristic excitation peaks of Er^{3+}. In the emission spectrum, the Cr^{3+} emission was highlighted by the diagonal shadow. (c) UCPL emission spectrum of ZGGO:Cr, Yb, Er recorded at 5 s after the stoppage of a 980 nm laser excitation. The upper right inset is the UCPL decay curve monitored at 700 nm emission. The left inset shows the NIR images (false color) taken at different delay times (5 min to 24 h) after ceasing the 980 nm laser excitation using a digital camera that was connected to the eyepiece of an ITT PVS-14 Gen III night vision monocular. The signals were attributed to the NIR UCPL. The imaging parameter is manual/ISO 400/30 s. For all the UCPL measurements, the samples were irradiated by a 980 nm laser for 10 min at a power of 600 mW.

the $3d$ excited energy levels of Cr^{3+} in the material, as indicated by the trap filling spectrum in Fig. S2 of the Supplemental Material [22]). As a result, after ceasing the 980 nm excitation, the gradual release of the captured electrons leads to NIR persistent luminescence from the Cr^{3+} ions (via the $^2E \rightarrow {}^4A_2$ transition).

The conceptual UCPL process illustrated in Fig. 2(a) was experimentally verified using spectral methods. Figure 2(b) shows the UCL emission bands of Er^{3+} ($^4S_{3/2} \rightarrow {}^4I_{15/2}$ and $^4F_{9/2} \rightarrow {}^4I_{15/2}$ transitions; yellow shadow area) and Cr^{3+} ($^2E \rightarrow {}^4A_2$ transition; diagonal shadow area) under a 980 nm laser excitation, as well as the excitation spectrum of ZGGO:Cr, Yb, Er by monitoring the 700 nm emission of Cr^{3+} (blue solid line curve). The spectral overlap between the Cr^{3+} excitation band and the Er^{3+} UCL emission bands suggests the excitability of Cr^{3+} by the 980 nm laser illumination via energy transfer [24]. The appearance of the Cr^{3+} photoluminescence band under 980 nm light excitation, as well as the appearance of Er^{3+} excitation peaks (at 519 and 640 nm as labeled by red dashed-line circles) in the excitation spectrum by monitoring the Cr^{3+} emission, verifies the occurrence of effective energy transfer between Er^{3+} and Cr^{3+} (note that without Er^{3+} codoping, $Zn_3Ga_2GeO_8$:1%Cr^{3+} or $Zn_3Ga_2GeO_8$:1%Cr^{3+}, 5%Yb^{3+} does not give Cr^{3+} luminescence under 980 nm light excitation, see Fig. S3 of the Supplemental Material [22]). The energy transfer between Er^{3+} and Cr^{3+} was further verified by the appearance of the up-conversion-induced Cr^{3+} persistent emission, i.e., the Cr^{3+} UCPL emission. Figure 2(c) shows the Cr^{3+} UCPL emission spectrum recorded immediately (the delay time is 5 s) after a 980 nm laser illumination (at 600 mW) for 10 min. The spectrum contains a strong emission band peaking at 700 nm (emission of Cr^{3+}) and a weak band peaking at 1010 nm (emission of Yb^{3+}, originating from the persistent energy transfer from Cr^{3+} to Yb^{3+}; the complete photoluminescence results are given in Fig. S4 of the Supplemental Material [22]). The upper inset of Fig. 2(c) shows the Cr^{3+} UCPL decay curve monitored at 700 nm after exposure to the 980 nm laser (600 mW) for 10 min. The data were recorded as a function of UCPL emission intensity versus time and the recording lasted for 60 min. After 60 min of persistent emission, the UCPL intensity was still significantly high, meaning that the UCPL should last much longer than 60 min. This long-lasting Cr^{3+} UCPL was verified by a NIR imaging experiment that utilized a night vision monocular (ITT PVS-14 Gen III) to monitor or image the changes of the emission "brightness" of a ZGGO:Cr, Yb, Er disk sample in a dark room, as the NIR images shown in the left inset of Fig. 2(c). After being exposed to the 980 nm laser for 10 min, the UCPL signals from the sample could be clearly visualized even after 24 h decay.

The results in Fig. 2(c) clearly show that low-energy 980 nm light excitation can result in higher-energy 700 nm (from Cr^{3+}) persistent luminescence via the up-conversion excitation channel in ZGGO:Cr, Yb, Er. To gain further insight about this new UCPL process, we studied the TL properties of ZGGO:Cr, Yb, Er under the excitation of a tunable 980 nm laser diode module (output power, 1–1000 mW), because the TL measurements can provide information related to the traps and the interactions between the Cr^{3+} ions and the traps [14,19,25]. Our previous study revealed that the traps were continuously distributed in the Cr^{3+}-activated ZGGO system [14], in which germanium was believed to play an important role in the formation of the high density of traps. According to the distribution characteristic of the traps in the Cr^{3+}-activated ZGGO system, we systematically tuned two excitation conditions in measuring the TL properties of the ZGGO:Cr, Yb, Er phosphor: varying the laser power (i.e., excitation intensity) between 200 and 700 mW with a fixed excitation duration of 300 s, and varying the excitation duration between 10 and 1000 s with a fixed laser power of 450 mW. Figure 3(a) shows a contour plot of the TL spectra acquired under the excitation of different laser powers between 200 and 700 mW in 50 mW steps

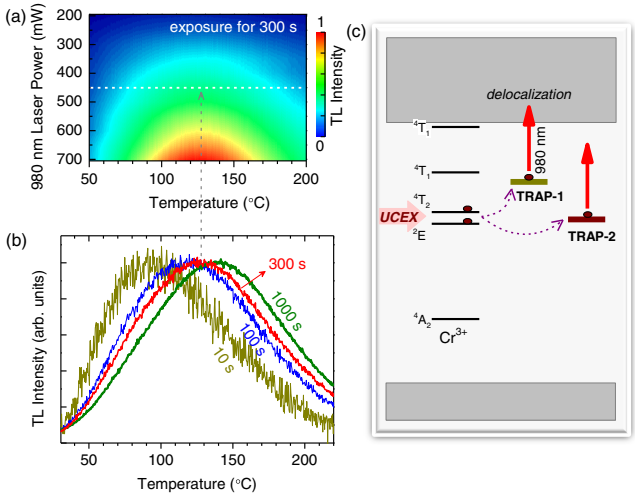

FIG. 3 (color online). (a) Contour plot of TL spectra obtained by illuminating a ZGGO:Cr, Yb, Er sample for 300 s with a 980 nm laser whose power was tuned between 200 and 700 mW. The monitoring wavelength is 700 nm. The magnitude of the TL intensity is shown by the color bar. (b) Normalized TL spectra obtained by illuminating a ZGGO:Cr, Yb, Er sample using a 980 nm laser (at 450 mW) for different exposure times from 10 to 1000 s. (c) Schematic representation of electron transfer under up-converted excitation (UCEX).

(the individual TL spectra are given in Fig. S5 of the Supplemental Material [22]). The TL intensity nonlinearly increases with the laser power (see the inset of Fig. S5(a) of the Supplemental Material [22]), but the position of the band maximum is independent of the laser power, which remains at ~128 °C. When the excitation duration varies, however, the position of the TL band maximum no longer remains constant. As shown in Fig. 3(b), the normalized TL peak position shifts from ~95 to ~138 °C when the excitation duration is increased from 10 to 1000 s (the laser power is kept at 450 mW), meaning that lengthening the excitation duration of the 980 nm laser changes the electron distribution in the traps. This observation is different from that commonly observed from high-energy light (UV and visible light) excited TL measurements in persistent phosphors, which show that in the same material, when the position of the TL band maximum is found to be independent of the excitation intensity, the same relationship should also occur with the excitation duration [25]. This phenomenon actually occurred in the present ZGGO:Cr, Yb, Er phosphor under the excitation of high-energy lights, e.g., a red light emitting diode (LED). That is, varying the excitation intensity (the variation range is 1000 times) and excitation duration (3 and 300 s) under a red LED excitation always produce the similar broad TL bands peaking at ~80 °C (i.e., no shift of the TL spectra), as shown in Fig. S6 of the Supplemental Material [22]. The TL maximum of 80 °C also coincides with that obtained after excitations with a wide range of excitation energies from UV to visible light [Fig. S2(a) of the Supplemental Material [22]].

The different TL behaviors in ZGGO:Cr, Yb, Er under the excitations of low-energy 980 nm light and high-energy UV or visible light indicate that the 980 nm illumination not only produces the up-converted excitation to fill the traps, but also influences the electron distribution in the traps. Based on the above results and discussions, we propose an electron transfer mechanism to account for the UCPL process in ZGGO:Cr, Yb, Er, as schematically shown in Fig. 3(c). To simplify the model, we divided the continuous traps into shallow traps (i.e., TRAP-1) and deep traps (i.e., TRAP-2). Under the excitation of a 980 nm laser, the up-converted excitation populates the $^4T_2/^2E$ crystal-field states of Cr^{3+}, followed by the filling of the shallow traps and deep traps in the material (it is worth noting that some details of the electron transfer, such as the possible change of the Cr valence state during the UCPL process, need to be investigated through suitable experimental techniques in the future). While the shallow traps are capturing electrons from the excited Cr^{3+}, the 980 nm excitation is also promoting the trapped electrons to the delocalized conduction band via a photostimulation process [19], resulting in the depopulation of electrons in the shallow traps. For the electrons in the deep traps, however, the 980 nm excitation energy is too low to promote them to the conduction band. Thus, the net population in the shallow traps increases more slowly than that in the deep traps as the excitation duration increases. As a result, the position of the TL band maximum shifts to higher temperature as the excitation duration increases [Fig. 3(b)]. This can also explain why the positions of the TL band maxima (~95–138 °C) under 980 nm light excitation [Fig. 3(b)] are higher than that (~80 °C) obtained under UV or visible light excitation (Figs. S2 and S6 of the Supplemental Material [22]; the high-energy UV or visible light has the same stimulation effects for the shallow and deep traps).

In conclusion, we have proposed a new UCPL concept by combining the unique features of the well-known UCL and LPL processes, and designed and fabricated the first UCPL phosphor $Zn_3Ga_2GeO_8:1\%Cr^{3+}$, $5\%Yb^{3+}$, $0.5\%Er^{3+}$ (ZGGO:Cr, Yb, Er) by incorporating a 5 mol%/0.5 mol% Yb^{3+}/Er^{3+} up-converting pair into the NIR LPL phosphor $Zn_3Ga_2GeO_8:1\%Cr^{3+}$. With the excitation of a 980 nm laser, besides the NIR UCPL emission from Cr^{3+}, the ZGGO:Cr, Yb, Er phosphor also exhibits effective UCL emissions from Er^{3+} and Cr^{3+}, even at low laser power (e.g., 20 mW; see Fig. S7 of the Supplemental Material [22]). Moreover, like its parent material $Zn_3Ga_2GeO_8:1\%Cr^{3+}$, the ZGGO:Cr, Yb, Er phosphor also exhibits a superior NIR persistent luminescence property from Cr^{3+} after excitation by UV (or visible) light (Fig. S8 of the Supplemental Material [22]). Such multimodal functions enable the ZGGO:Cr, Yb, Er phosphor to find applications in many important

areas, particularly in biomedical imaging that requires high sensitivity, a long observation window, a deep tissue penetration depth, and excitability *in vivo*. Finally, the UCPL concept is general and can be used to design many other new UCPL materials based on existing persistent phosphors. For example, by incorporating 10 mol %/0.5 mol % Yb^{3+}/Tm^{3+} into $La_3Ga_5GeO_{14}:2\%Cr^{3+}$ [26], we obtained the $La_3Ga_5GeO_{14}:2\%Cr^{3+}$, $10\%Yb^{3+}$, $0.5\%Tm^{3+}$ UCPL material exhibiting broadband Cr^{3+} UCPL emission after excitation with a 980 nm laser (Fig. S9 of the Supplemental Material [22]).

This work is supported by the U.S. National Science Foundation (NSF CAREER DMR-0955908). Y. L. acknowledges support from the China Scholarship Council.

*panz@uga.edu

[1] F. Auzel, Chem. Rev. **104**, 139 (2004).
[2] X. Huang, S. Han, W. Huang, and X. Liu, Chem. Soc. Rev. **42**, 173 (2013).
[3] S. Heer, K. Kömpe, H.-U. Güdel, and M. Haase, Adv. Mater. **16**, 2102 (2004).
[4] S. Heer, O. Lehmann, M. Haase, and H.-U. Güdel, Angew. Chem., Int. Ed. Engl. **42**, 3179 (2003).
[5] E. Downing, L. Hesselink, J. Ralston, and R. Macfarlane, Science **273**, 1185 (1996).
[6] D. Matsuura, Appl. Phys. Lett. **81**, 4526 (2002).
[7] M. Haase and H. Schafer, Angew. Chem., Int. Ed. Engl. **50**, 5808 (2011).
[8] J. Hölsä, Electrochem. Soc. Interface **18**, 42 (2009).
[9] P. Dorenbos, J. Electrochem. Soc. **152**, H107 (2005).
[10] J. Hölsä, T. Aitasalo, H. Jungner, M. Lastusaari, J. Niittykoski, and G. Spano, J. Alloys Compd. **374**, 56 (2004).
[11] H. Yamamoto and T. Matsuzawa, J. Lumin. **72–74**, 287 (1997).
[12] T. Matsuzawa *et al.*, J. Electrochem. Soc. **143**, 2670 (1996).
[13] X. Wang, Z. Zhang, Z. Tang, and Y. Lin, Mater. Chem. Phys. **80**, 1 (2003).
[14] Z. W. Pan, Y. Y. Lu, and F. Liu, Nat. Mater. **11**, 58 (2012).
[15] D. K. Chatterjee, A. J. Rufaihah, and Y. Zhang, Biomaterials **29**, 937 (2008).
[16] F. Wang, D. Banerjee, Y. Liu, X. Chen, and X. Liu, Analyst (Cambridge, United kingdom) **135**, 1839 (2010).
[17] J. Zhou, Z. Liu, and F. Y. Li, Chem. Soc. Rev. **41**, 1323 (2012).
[18] Q. L. de Chermont, C. Chaneac, J. Seguin, F. Pelle, S. Maitrejean, J.-P. Jolivet, D. Gourier, M. Bessodes, and D. Scherman, Proc. Natl. Acad. Sci. U.S.A. **104**, 9266 (2007).
[19] F. Liu, W. Yan, Y.-J. Chuang, Z. Zhen, J. Xie, and Z. Pan, Sci. Rep. **3**, 1554 (2013).
[20] T. Maldiney, G. Sraiki, B. Viana, D. Gourier, C. Richard, D. Scherman, M. Bessodes, K. Van den Eeckhout, D. Poelman, and P. F. Smet, Opt. Mater. Express **2**, 261 (2012).
[21] J.-H. Park, L. Gu, G. von Maltzahn, E. Ruoslahti, S. N. Bhatia, and M. J. Sailor, Nat. Mater. **8**, 331 (2009).
[22] See Supplemental Material at http://link.aps.org/supplemental/10.1103/PhysRevLett.113.177401 for Figs. S1 to S9.
[23] W. Jia, K.-S. Lim, H. Liu, Y. Wang, F. Fernandez, and W. M. Yen, J. Lumin. **66–67**, 228 (1995).
[24] D. L. Dexter, J. Chem. Phys. **21**, 836 (1953).
[25] K. Van den Eeckhout, A. J. J. Bos, D. Poelman, and P. F. Smet, Phys. Rev. B **87**, 045126 (2013).
[26] W. Yan, F. Liu, Y.-Y. Lu, X.-J. Wang, M. Yin, and Z. Pan, Opt. Express **18**, 20215 (2010).